Valence Band Electronic Structures of Heavily Boron-Doped Superconducting Diamond Studied by Synchrotron Photoemission Spectroscopy

Takayoshi Yokoya[1,2*], Tetsuya Nakamura[2], Tomohiro Matsushita[2],
Takayuki Muro[2], Eiji Ikenaga[2], Masaaki Kobata[2], Keisuke Kobayashi[2],
Yoshihiko Takano[3], Masanori Nagao[3], Tomohiro Takenouchi[4],
Hiroshi Kawarada[4] and Tamio Oguchi[5]

[1]The Graduate School of Natural Science and Technology, Okayama University,
3-1-1 Tsushima-naka, Okayama 700-8530, Japan
[2]Japan Synchrotron Radiation Research Institute (JASRI)/SPring-8,
1-1-1 Kouto, Sayo, Hyogo 679-5198, Japan
[3]National Institute for Material Science, 1-2-1 Sengen, Tsukuba, Ibaraki 305-0047, Japan
[4]School of Science and Engineering, Waseda University,
3-4-1 Okubo, Shinjuku, Tokyo 169-8555, Japan
[5]Department of Quantum Matter, Graduate School of Advanced Sciences of Matter (ADSM),
Hiroshima University, 1-3-1 Kagamiyama, Higashi-Hiroshima 739-8530, Japan

The valence band electronic structures of heavily boron-doped superconducting diamond films made by microwave plasma-assisted chemical vapor deposition (MPCVD) were investigated by hard X-ray photoemission spectroscopy (HXPES) and soft X-ray angle-resolved photoemission spectroscopy (SXARPES). The HXPES core-level spectrum of heavily boron-doped diamond shows a new feature at the lower binding energy side of the C 1s main peak. The HXPES valence band spectrum of a heavily boron-doped superconducting diamond film shows a broader spectral shape than that of a lightly doped non-superconducting sample. The SXARPES results of homoepitaxial CVD films show clear valence band dispersions with a bandwidth of ~23 eV and the top of the valence band at the Γ point in the Brillouin zone, which are well explained by the calculated valence band dispersions of pure diamond. Boron concentration-dependent band dispersions near the Fermi level (E_F) by SXARPES exhibit a systematic shift in E_F,

---

*Corresponding author: e-mail: yokoya@cc.okayama-u.ac.jp

indicating electron depopulation due to hole doping, and an increase in the line shape corresponding to the broader density of states observed by HXPES. These results indicate that holes in the top of the valence band are responsible for the metallic states leading to superconductivity at low temperatures. The HXPES C 1s core-level spectra of lightly boron-doped non-superconducting and heavily boron-doped superconducting films are also shown.

1. Introduction

Recently, Ekinov *et al.* have reported that heavily boron-doped diamond, made using a high-pressure and high-temperature synthesis process, exhibits superconductivity below a transition temperature of ~4 K.[1] Reproducibility was confirmed with films made by microwave plasma-assisted chemical vapor deposition (MPCVD)[2,3] and a transition temperature (T_c) of 11.4 K was achieved in a MPCVD film.[4] Technologically, diamond has outstanding properties, including hardness, a high thermal conductivity, and a wide band gap, and is regarded as a very promising semiconductor.[5] Superconductivity adds another functionality, which might lead to new diamond-related devices when combined with other properties. For developing new diamond-based devices and/or to understand their characteristics, electronic structure diagrams provide fundamental information, as in those of lightly doped semiconductor devices.[6] Thus, the electronic structure of heavily boron-doped diamond is important for the development of new diamond devices. Scientifically, how an insulator with a wide band gap becomes a metal by doping has not been experimentally proven to date and therefore is a fundamental question.[7] Indeed, depending on the origin of the metallic states, different approaches to clarify the mechanism of superconductivity have been proposed.[8–12]

In diamond, carbon atoms are crystallized into a C $2s2p^3$ 3-dimensional network (Fig. 3(a)) with covalent bonding. The resulting band structure has a large valence band width (22 eV), whose top, located at the Γ point in the Brillouin zone (BZ), is separated from the bottom of the conduction band by a 5.5 eV band gap.[13] For a low carrier concentration, boron atoms most probably replace the carbon sites substitutionally and form an impurity level having an activation energy of 0.37 eV.[14] As the boron concentration is increased, the wave functions of holes bound to an impurity site can overlap and the impurity level evolves into an impurity "band." The holes in a nearly localized "band" strongly experience Coulomb forces due to small screening effects; thus, electron-electron correlation plays an important role. This possibility was pointed out, along with a prediction of an extended s-wave superconductivity due to electron correlation.[8] This is an approach from a localized picture evolving into a metallic state in the vicinity of the semiconductor-metal transition. On the other hand, one can foresee an extended picture for the metallic states. In this case, we start from the

diamond band structure. The doped holes lead to the depopulation of the bands with a predominant diamond character hybridized with boron states. Recent theoretical studies based on band structure calculations predicted that superconductivity is driven by phonons strongly coupled to holes at the Γ point.[8–11]

Thus, an accurate description of the overall valence band electronic structure is extremely important for understanding the mechanism of superconductivity, as well as for the future development of new diamond devices. In addition, core-level photoemission spectroscopy may shed light on boron-doping-induced electronic structures, which are essential for understanding local bonding. In this article, we present valence band and core-level electronic structures studied by hard X-ray photoemission spectroscopy (HXPES) and soft X-ray angle-resolved photoemission spectroscopy (SXARPES).[15]

2.   Experimental Method

Polycrystalline lightly and heavily boron-doped diamond films for HXPES were prepared using MPCVD as described elsewhere.[2] A T_c of 3 K for the superconducting film was measured by magnetization measurements. Homoepitaxially grown heavily boron-doped (111) diamond films for SXARPES (BDD1, BDD2 and BDD3) were made using MPCVD as described elsewhere.[4] A T_c of 7.0 K for BDD3 was confirmed at the onset of magnetization measurements after the present photoemission measurements. The T_c determined from the onset of magnetization measurements was lower than that determined from the onset of resistivity measurements and normally corresponded to zero resistivity. BDD2 and BDD1 did not show an onset of magnetization measurements above 1.7 K. However, BDD2 showed an onset of resistivity measurements below 2.5 K. Secondary ion mass spectroscopy (SIMS) measurements for BDD1, BDD2, and BDD3 made using the same conditions as those used for the samples we used gave boron concentrations of 2.88×10^{20}, 1.18×10^{21}, and 8.37×10^{21} cm^{-3}, respectively.

HXPES measurements were performed at BL29XU, SPring-8, on a spectrometer built using a modified Scienta SES2002 electron analyzer.[16] Measurements were performed using an angle-integrated mode with a total energy resolution of ~250 meV for a photon energy of 5994 eV at 20 K. No surface treatment was carried out prior to measurements. SXARPES measurements were performed at BL25SU, SPring-8, on a spectrometer built using a Scienta SES200 electron analyzer. The energy and angular resolution were set to ~250 meV and ±0.1° (corresponding to ±0.026 Å^{-1}) for a photon energy of 825 eV, respectively, to obtain a reasonable count rate. Samples were cooled using a closed-cycle He refrigerator. Sample T was measured using a chromel-AuFe thermocouple mounted close to the sample. The base pressure of the spectrometer was better than 3×10^{-8} Pa. The sample orientation was measured *ex situ* using Laue photography. The location of the Γ point with respect to the measured ARPES data and the E_F position in the calculated spectra were determined by comparing the experimental and calculated band dispersions near E_F. All measurements were performed for surfaces prepared by annealing at 400°C to reduce oxygen contamination

at the surface. The E_F of the samples was referenced to that of a gold film evaporated onto the sample substrate measured just after the sample measurements were performed. The measured k positions were determined using a free-electron final state model by the equation $\hbar k = [2m(E\cos2\theta+V_0)]^{1/2} - k_{photon}$, where $\hbar$ is Planck's constant, m is the electron mass, E and θ are the kinetic energy and polar angle of an emitted photoelectron, respectively, V_0 is the inner potential, and k_{photon} is the surface normal momentum component of a photon. In the present case we used a V_0 of 23 eV.

3.   Results and Discussion

Figure 1 shows the HXPES C 1s core-level spectra of lightly boron-doped non-superconducting and heavily boron-doped superconducting diamonds measured at 20 K with a photon energy of 5994 eV. We found that both C 1s spectra exhibit a prominent peak, whose energy positions shift to a lower binding energy as boron concentration is increased. We also found that the main peak of each spectra is accompanied by a tail, which is most probably composed of several components, at a higher binding energy that was found to have a strong sample dependence[17] and therefore originated from extrinsic nature most probably derived from oxide contamination at the surface and/or grain boundary.[18] Importantly, the C 1s spectrum of the heavily boron-doped superconducting film has a foot structure at the lower binding energy side of the main peak at approximately 282.5 eV, which is absent in that of the lightly doped sample. This additional lower binding energy feature of the C 1s spectra of diamond in carbon
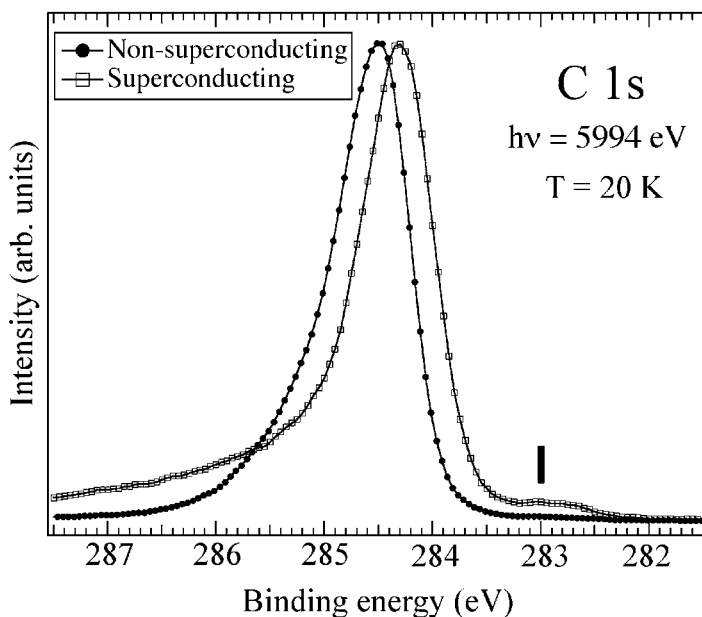

Fig. 1.   HXPES C 1s core-level spectra of lightly doped non-superconducting and heavily doped superconducting diamonds measured at 20 K with photon energy of 5994 eV.

films was ascribed to bonding with sp^2 configuration.[19,20] In contrast, we found that the intensity of the additional feature at approximately 282.5 eV shows boron concentration dependence,[17] which indicates a close correlation between the new feature and the boron concentration. Note that band structure calculations using a supercell have predicted a longer bond length between the doped boron and the nearest neighboring C atoms,[11] which can change the energy of the C 1s core level.

In Fig. 2, we plotted the HXPES valence band spectra of lightly boron-doped non-superconducting and heavily boron-doped superconducting diamonds measured at 20 K with a photon energy of 5994 eV. The spectrum of the lightly boron-doped diamond shows three structures at 9.5, 13, and 17.5 eV. The spectral shape is found to be consistent with those of previous reports;[19,20] thus, the three structures can be assigned as being in p, sp, and s dominant states, respectively. The valence band spectrum of the heavily boron-doped superconducting diamond was found to be broader than that of the lightly boron-doped diamond, but the three structures seem to be retained with heavy boron doping.

To study the valence band electronic structure in more detail, we used SXARPES wherein momentum-dependent electronic states, namely, the band dispersion of solids, can be directly observed. Figures 3(c) and 3(d) show the SXARPES intensity maps of BDD1 and BDD2 along the gray curve in the ΓKLUX plane of BZ (Fig. 3(b)) using
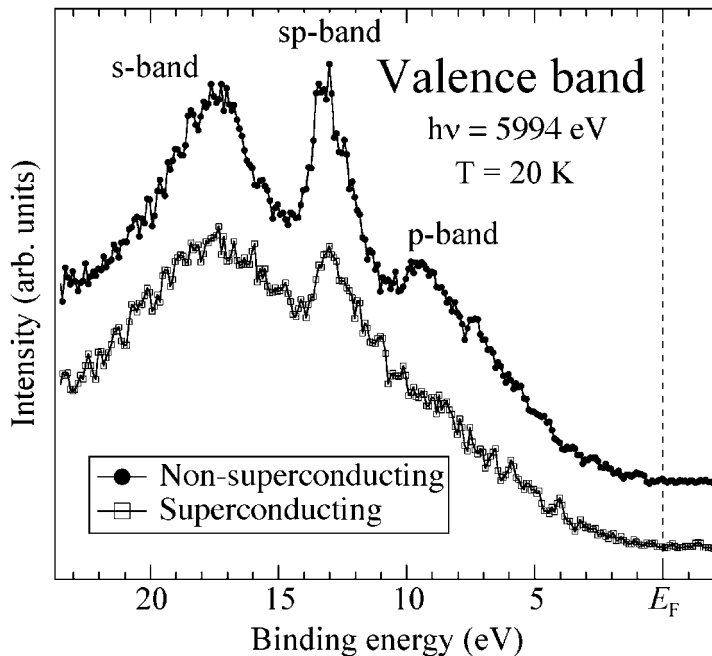

Fig. 2. HXPES valence band spectra of lightly doped non-superconducting and heavily doped superconducting diamonds measured at 20 K with photon energy of 5994 eV.
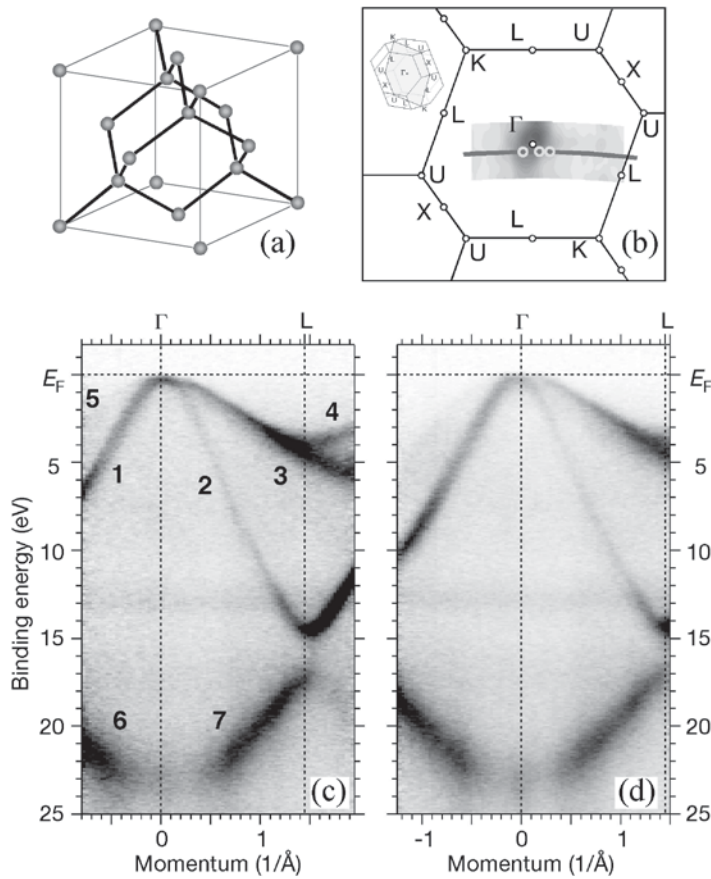
Fig. 3. (a) Conventional unit cell of diamond. (b) Two-dimensional BZ showing estimated measured k positions for states near E_F with gray curve. The inset shows 3-dimensional BZ. (c) and (d) Valence band SXARPES intensity maps from single-crystal diamond (111) film (BDD1 and BDD2) using photon energy of 825 eV along gray curve in (b). Higher spectral intensity corresponds to darker color.

a photon energy of 825 eV . In Fig. 3(c), several dispersive features corresponding to experimentally obtained bands can be observed, as denoted by 1–7. For the lower binding energy region, we clearly observed four dispersive features (1–4). Band 4 seems to merge into band 3 for lower momentum. One can observe a faint but dispersive feature at 5, the corresponding dispersive feature of which may be more clearly observed in Fig. 3(d). Bands 1–4 disperse toward E_F and appear to exist very near E_F at Γ (we will discuss the band dispersion near E_F in detail later). Band 2 has an energy bottom at a binding energy of 14 eV and at approximately 1.5 Å^{-1}. At higher binding energy

regions, we observed higher intensity features at both sides of Γ (6 and 7), suggesting a parabolic dispersion having a bottom at Γ. Band 7 seems to have their top of dispersion at approximately 1.5 Å^{-1}, forming a band gap with Band 2 at a zone boundary. We found that these bands are very similar to the calculated band dispersions of pure diamond,[15] but the experimental band width (23.5 ± 0.5 eV) is wider than that of the calculations (21.5 eV). For BDD2, the observed band dispersions are similar to those of BDD1. These indicate that the valence band dispersions of diamond are retained by boron doping.

As mentioned above, we found that the highly dispersive bands approach very near to E_F as shown in Figs. 3(c) and 3(d). To more carefully observe the states near E_F and its boron concentration dependence, we further performed SXARPES measurements for BDD1, BDD2, and BDD3 with a smaller step size and a higher signal to noise ratio, as shown in Figs. 4(a)–4(c). For BDD1, we clearly observe three bands near E_F (1, 2, and 3) and find that bands 1 and 2 form a parabolic-like dispersion having an energy and intensity maximum at $k = 0$ and near E_F. As the boron concentration increases, the intensity of the top of the parabolic-like band decreases and the intensity maps of BDD2
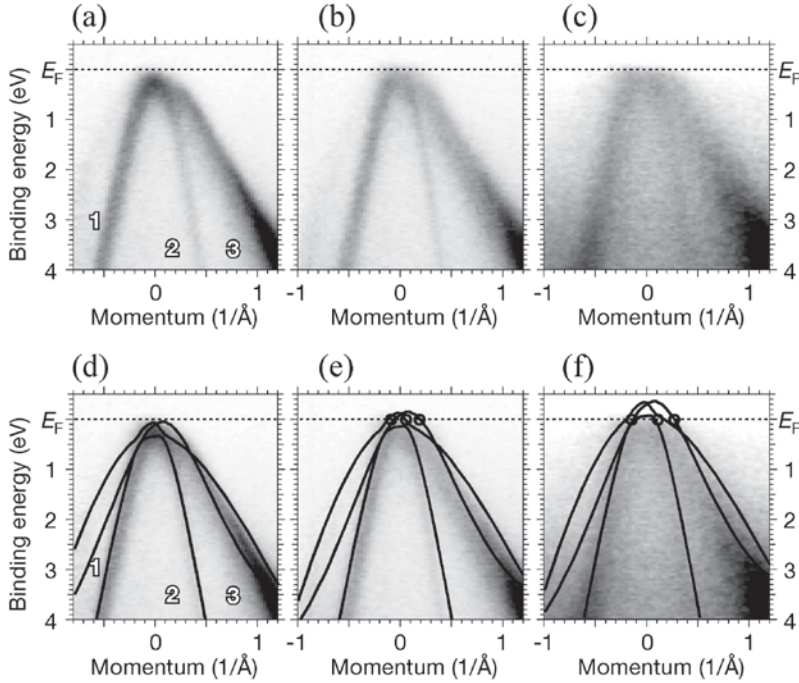

Fig. 4. (a), (b), and (c): Near E_F SXARPES intensity maps from single-crystal diamond (111) film (BDD1, BDD2, and BDD3) using photon energy of 825 eV along gray curve in Fig. 3(b). (d), (e), and (f): The same as (a), (b), and (c) superimposed with valence band dispersions of pure diamond. Circles at E_F denote k_F's.

and BDD3 show local minima at the Γ-point. For BDD3, the top of the parabolic-like band appears to be truncated, which indicates the introduction of holes in the top of the valence band. Moreover, the bands of BDD3 are vaguer than those of BDD1 and BDD2, suggesting broadened electronic structures in BDD3. This is consistent with the broadened electronic structure of heavily boron-doped superconducting diamond as experimentally observed by HXPES and as theoretically predicted from band structure calculations.[21]

From the momentum distribution curves, Fermi momenta were determined for BDD3 ($k_F^1 = -0.15 \pm 0.04$ Å^{-1}, $k_F^2 = 0.11 \pm 0.02$ Å^{-1}, and $k_F^3 = 0.27 \pm 0.02$ Å^{-1}) and for BDD2 ($k_F^1 = -0.09 \pm 0.01$ Å^{-1}, $k_F^2 = 0.06 \pm 0.008$ Å^{-1}, and $k_F^3 = 0.19 \pm 0.007$ Å^{-1}). We also found the location of E_F at 0.40 ± 0.2 eV (0.2 ± 0.1 eV) below the top of the valence band as shown in Fig. 4(f) (4(e)) corresponding to the region of the carrier concentration, i.e., $6.6 \times 10^{20} < n = 1.9 \times 10^{21}$ cm$^{-3} < 4.4 \times 10^{21}$ cm^{-3} for BDD3 ($6 \times 10^{19} < n = 6.6 \times 10^{20}$ cm$^{-3} < 9.8 \times 10^{20}$ cm^{-3} for BDD2). Note that the carrier concentrations estimated from the SXARPES measurements are slightly lower than the B concentrations from the SIMS measurements.

These results indicate that doped holes enter into the top of a valence band, accompanied by a shift in E_F. This is in agreement with the predictions from band structure calculations.[9–12,21]   The experimental observation that E_F locates at the top of the valence band with highly dispersive bands, but not at independent nondispersive impurity bands, may also provide important information for the future development of diamond-based devices.[5]

4.   Summary

Boron-concentration-dependent core-level and valence band electronic states of boron-doped diamond have been studied by HXPES and SXARPES. The C 1s spectrum of heavily boron-doped diamond shows new lower binding energy features. By SXARPES, a systematic shift in E_F with respect to diamond valence band was observed. This indicates that heavy boron doping induces holes in the top of a valence band, which can be expected to couple with high-frequency phonons and thus induce superconductivity from band structure calculations. The present results revealed that an overall occupied electronic structure directly relates to the metallicity of a heavily boron-doped diamond superconductor. An understanding of the electronic structure of a heavily boron-doped diamond may also be important for developing possible diamond-based devices utilizing the unique properties of diamond.

Acknowledgements

References

1) E. A. Ekimov, V. A. Sidorov, E. D. Bauer, N. N. Mel'nik, N. J. Curro, J. D. Thompson and S. M. Stishov: Nature **428** (2004) 542.
2) Y. Takano, M. Nagao, I. Sakaguchi, M. Tachiki, T. Hatano, K. Kobayashi, H. Umezawa and H. Kawarada: Appl. Phys. Lett. **85** (2004) 2851.
3) E. Bustarret, F. Gheeraert and K. Watanabe: Phys. Rev. Lett. **93** (2004) 237005.
4) H. Umezawa *et al*.: cond-mat/0503303.
5) C. E. Nebel and J. Ristein: *Thin-film diamond II* (Elsevier B.V., Amsterdam, 2004).
6) N. W. Ashcroft and N. D. Mermin: *Solid State Physics* (Saunders College Publishing, Fortworth, 1976).
7) J. Kortus: Nature Materials **4** (2005) 879.
8) G. Baskaran: cond-mat/0404286.
9) L. Boeri, J. Kortus and O. K Andersen: Phys. Rev. Lett. **93** (2004) 237002.
10) K.-W. Lee and W. E. Pickett: Phys. Rev. Lett. **93** (2004) 237003.
11) X. Blasé, Ch. Adessi and D. Connetable: Phys. Rev. Lett. **93** (2004) 237004.
12) H. J. Xiang, Z. Li, J. Yamg, J. G. Hou and Q. Zhu: Phys. Rev. B **70** (2004) 212504.
13) J. R. Chelikowsky and S. G. Louie: Phys. Rev. B **29** (1984) 3470.
14) A. T. Collins and A. W. S. Williams: J. Phys. C: Solid State Phys. **4** (1971) 1789.
15) T. Yokoya, T. Nakamura, T. Matsushita, T. Muro, Y. Takano, M. Nagao, T. Takenouchi, Y. Kawarada and T. Oguchi: Nature **438** (2005) 647.
16) K. Kobayashi, M. Yabashi, Y. Takata, T. Tokushima, S. Shin, K. Tamasaku, D. Miwa, T. Ishikawa, H. Nohira, T. Hattori, Y. Sugita, O. Nakatsuka, A. Sakai and S. Zaima: Appl. Phys. Lett. **83** (2003) 1005.
17) T. Yokoya *et al.*: submitted to Phys Rev. B.
18) J. I. B. Wilson, J. S. Walton and G. Beamson: J. Electron Spectroscopy and Related Phenomena **121** (2001) 183.
19) F. R. McFeely, S. P. Kowalczyk, L. Ley, R. G. Cavell, R. A. Pollak and D. A. Shirley: Phys. Rev. B **9** (1974) 5268.
20) R. G. Cavell, S. P. Kowalczyk, L. Ley, R. A. Pollak, B. Mills, D. A. Shirley and W. Perry: Phys. Rev. B **7** (1973) 5313.
21) K.-W. Lee and W. E. Pickett: Phys. Phys. Rev. B **73** (2006) 075105.